Spectroscopic Studies on Bioactive Polyacetylenes and Other Plant Components in Wild Carrot Root

ARTICLE *in* JOURNAL OF NATURAL PRODUCTS · JULY 2011

Impact Factor: 3.8 · DOI: 10.1021/np200265d · Source: PubMed

4 AUTHORS, INCLUDING:

Maciej Roman
Polish Academy of Sciences
12 PUBLICATIONS **69** CITATIONS
SEE PROFILE

Malgorzata Baranska
Jagiellonian University
159 PUBLICATIONS **1,866** CITATIONS
SEE PROFILE

Rafal Baranski
University of Agriculture in Krakow
48 PUBLICATIONS **584** CITATIONS
SEE PROFILE

JOURNAL OF NATURAL PRODUCTS

ARTICLE

pubs.acs.org/jnp

Spectroscopic Studies on Bioactive Polyacetylenes and Other Plant Components in Wild Carrot Root

Maciej Roman,[†] Jan Cz. Dobrowolski,[‡,§] Malgorzata Baranska,[†] and Rafal Baranski*[,⊥]

[†]Faculty of Chemistry, Jagiellonian University, 3 Ingardena Street, 30-060 Krakow, Poland

[‡]Spectroscopy and Molecular Modeling Group, Industrial Chemistry Research Institute, 8 Rydygiera Street, 01-793 Warsaw, Poland

[§]Laboratory of Theoretical Methods and Calculations, National Medicines Institute, 30/34 Chełmska Street, 00-725 Warsaw, Poland

[⊥]Department of Genetics, Plant Breeding and Seed Science, Faculty of Horticulture, University of Agriculture in Krakow, Al. 29 Listopada 54, 31-425 Krakow, Poland

ABSTRACT: Polyacetylenes and other common plant components, such as starch, pectin, cellulose, and lignin, were studied in roots of the wild carrot (*Daucus carota*) subspecies *D. carota* subsp. *gummifer* and *D. carota* subsp. *maximus* by Raman spectroscopy. The components were measured *in situ*, directly in the plant tissue and without any preliminary sample preparation. The analysis was performed on the basis of the intense and characteristic key bands observed in the Raman spectrum. The two main carrot polyacetylenes falcarinol (**1**) and falcarindiol (**2**) have similar molecular structures, but their Raman spectra exhibit a small band shift in the symmetric −C≡C−C≡C− mode from 2258 cm^{-1} to 2252 cm^{-1}. Quantum chemical calculations confirmed that the differences observed between the samples may be due to conformational and environmental changes. The polyacetylenes were also detected by Raman mapping, which visualized the distribution of the compounds across sections of carrot roots. The mapping technique was also applied to assess the distribution of lignin and polysaccharide compounds. The results showed the tissue-specific accumulation of starch and cell wall components such as lignin, pectin, and cellulose.

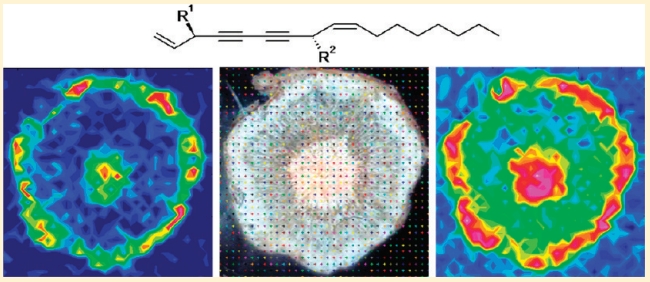

Edible carrot (*Daucus carota* subsp. *sativus* Hoffm.) belongs to the Apiaceae family, one of the largest plant families, which also comprises important vegetable and condiment species such as celery, celeriac, parsnip, parsley, fennel, dill, coriander, and caraway. *Daucus carota* is comprised of six to 11 subspecies depending on the taxonomic division used.[1,2] Among the wild *D. carota* subspecies, *D. carota* subsp. *gummifer*, a naturally occurring variant found along the European Atlantic coast, and *D. carota* subsp. *maximus*, which is distributed in the Mediterranean region, are the most represented in European and American gene banks, with collections of 10 and 38 accessions of each subspecies, respectively. The plants of both subspecies develop a white storage root, although much smaller than that of the commercial edible carrot.[2]

Health-promoting properties of fruits and vegetables have recently been attributed to the presence of secondary metabolites that demonstrate bioactivity. Some secondary metabolites are unwanted in the human diet due to their toxic effects at high concentrations; however, they may be beneficial at low concentrations. This phenomenon is called hormesis, or the biphasic effect, and it is observed in the case of polyacetylenes.[6−8] These compounds are neurotoxic and function as potent skin sensitizers at high concentrations. Falcarinol (**1**) and falcarindiol (**2**) are the most common polyacetylenes in edible plants and also exhibit beneficial properties at low concentrations. Both polyacetylenes demonstrate antifungal activity,[9,10] anti-inflammatory and antiplatelet-aggregatory properties,[11,12] and antibacterial effects at nontoxic concentrations.[13] Polyacetylenes are also known to be inhibitors of enzymes such as diacylglycerol acyltransferase,[14] inducible nitric oxide synthase,[15,16] and cholesteryl ester transfer protein,[17] as well as microsomal and mitochondrial enzymes.[18] Additionally, polyacetylenes are highly cytotoxic against numerous cancer cell lines *in vitro*, e.g., human gastric adenocarcinoma.[19,20]

The presence of falcarinol-type polyacetylenes is characteristic for plants of the Apiaceae and Araliaceae families.[4] The two polyacetylenes **1** and **2** occur in cultivated vegetables such as carrot, parsley, celeriac, and parsnip. Both compounds have two conjugated triple bonds, −C≡C−C≡C−, but they differ by the presence of one additional hydroxy group in **2**. They are accompanied by a derivate of **2**, 3-*O*-acetylfalcarindiol (**3**), which can contribute between 25% and 50% of the total polyacetylene content. The level of polyacetylenes is also postulated to strongly influence the bitter off-taste of fresh and stored food plants. For instance, the bitterness of carrot roots is reported to be predominantly caused by **2**.[21,22]

The concentration of polyacetylenes in food plants is low and usually ranges from 20 to 100 mg kg^{-1} fresh weight (FW).[23] However, the level of polyacetylenes can increase as an induced plant response to pathogen invasion.[9,10,24] In carrot root, the concentration of the most abundant **2** is highly genotype dependent and varies from 16 to 84 mg kg^{-1} FW; in contrast, **1** occurs in amounts of 5−41 mg kg^{-1} FW.[21,22,25] The distribution of polyacetylenes in a root is not homogeneous. The highest

Received: March 28, 2011
Published: July 29, 2011

concentration of **2** was found in the basal (upper) part of the root in phloem tissue. In fact, the peel as well as greening and dark colored spots of carrot root tissues contain higher concentrations of this compound.[22] In the closest wild relative subspecies (*D. carota* subsp. *carota*) the content of **2** may be higher (583 mg kg^{-1} dry weight; DW) and that of **1** lower (399 mg kg^{-1} DW) than those in edible carrots (82−518 mg kg^{-1} DW and 236−1553 mg kg^{-1} DW, respectively). However, only one locally grown wild carrot accession was used, whereas a range of edible carrots of different origin and root color were selected.[23] Other *D. carota* subspecies may contain even a few times higher concentrations of polyacetylenes; however, the plants are fragile and usually do not develop storage roots. Unlike most subspecies, the size of *D. carota* subsp. *maximus* and *D. carota* subsp. *gummifer* plants is similar to that of edible carrot, and their storage roots accumulate polyacetylenes up to 2000 mg kg^{-1} FW, with **2** being the main compound.[26]

Besides valuable polyacetylenes, carrot roots contain some key components such as lignin and polysaccharides such as cellulose, pectin, and starch. Their amount and distribution differ between cultivars and reflect the quality of the product. Moreover, during processing or storage steps, these components may undergo some structural changes, which may substantially influence the final taste and consistency of the vegetable.[27]

The identification and quantitative determination of secondary metabolites in food plants are usually performed using chromatographic methods that require destructive plant material compound extraction.[21,22,28,29] This makes it impossible to investigate compound distribution at the cellular level. However, this limitation can be overcome by the use of Raman spectroscopy, a technique that has been successfully applied for the nondestructive investigation of natural compounds, e.g., carotenoids[30,31] or essential oils,[32] in various plants. The simultaneous determination of several components *in situ* is possible when using the Raman mapping technique, as exemplified for polyacetylenes, carotenoids, and polysaccharides in carrot, as well as ginseng and *Bidens ferulifolia* samples.[5,33−35] The latter investigations also recorded root measurements of wild carrot *D. carota* subsp. *maritimus*, where **2**, starch, and pectin were detected.[5]

Two subspecies, *D. carota* subsp. *maximus* and *D. carota* subsp. *gummifer*, can be considered as valuable sources of polyacetylenes, as they develop relatively big storage roots rich in **2**. However, the distribution of secondary metabolites in plant tissues may depend on the taxa even if they belong to the same species.[5] This work was commenced to determine whether the polyacetylene distribution in roots of two wild carrots is tissue dependent and what tissue is the most valuable source of these compounds. We applied FT-Raman mapping technique for the simultaneous investigation of polyacetylenes together with pectin, starch, lignin, and cellulose in root cross sections that enabled visualization of tissue-dependent distribution without the need for compound extraction. We also performed quantum chemical calculations for **1** and **2** to discuss the influence of the plant matrix on the conformation of polyacetylenes and consequently on the position of their characteristic marker bands.

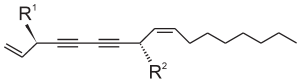

1 R^1 = OH, R^2 = H
2 R^1 = R^2 = OH
3 R^1 = $OCOCH_3$, R^2 = OH

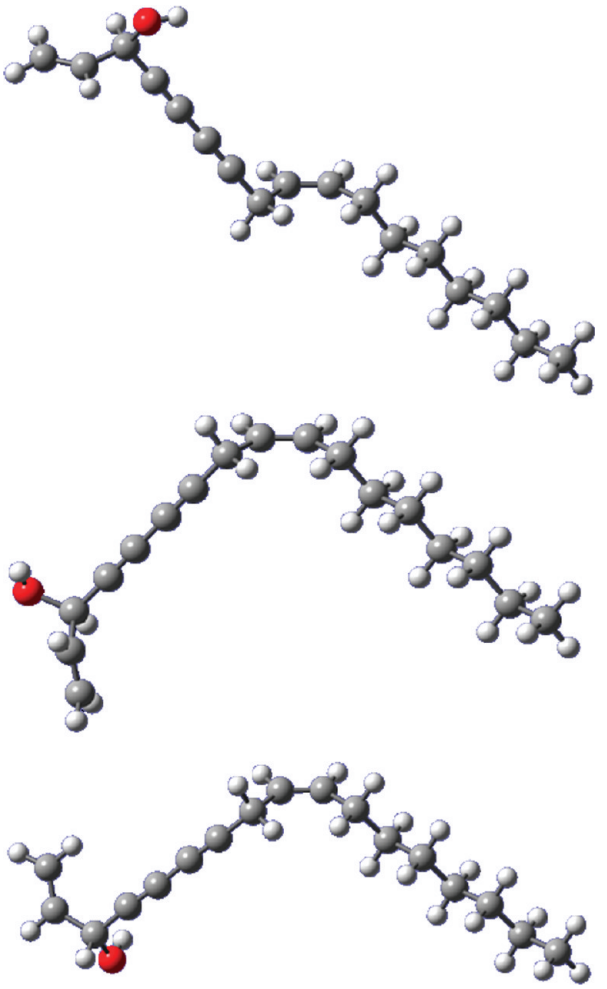

Figure 1. Structure of exemplary conformers of **1** obtained from conformational analysis using quantum chemical calculations.

RESULTS AND DISCUSSION

Influence of Conformation and Environment on the Spectroscopic Properties of 1 and 2. Inspecting the presence of polyacetylenes in a plant by means of Raman spectroscopy is relatively easy given the occurrence of strong and polarized bands that are due to the symmetric stretch of the triple-bond system in the region of about 2200 cm^{-1}.[5,33−35,40] Since only a few oscillators absorb in that specific region, the analysis of polyacetylene bands is reliable. However, small differences in the band position can be observed in the spectra of plant materials containing **1** and **2**, and their origin has not been explained yet. This may be due to the variety in conformations of polyacetylene molecules or structural changes caused by the plant matrix. To investigate this problem, the spectroscopic properties of **1** and **2** conformers were studied using theoretical calculations. This approach was successfully applied for the analysis of natural monoacetylenes when experimental data were limited.[41]

The results of vibrational frequency calculations and geometry optimization for the conformers of **1** and **2** (Figure 1) calculated for the gas phase are presented in Table 1. The positions of both triple-bond stretching vibration modes [ν_{as}(C≡C) and ν_s(C≡C)] in the conformations of **1** and **2** vary within less than 10 and 20 cm^{-1}, respectively. The range of calculated frequencies

Table 1. IR and Raman Spectra Parameters of the ν_{as}(C≡C) and ν_s(C≡C) Bands of the 1 and 2 Conformers Calculated at the B3LYP/aug-cc-pVDZ Level[a]

polyacetylene	environment	ν_{as} (C≡C) (cm^{-1})	I_{IR} (km mol^{-1})	A_R (A^4 amu^{-1})	ν_s (C≡C) (cm^{-1})	I_{IR} (km mol^{-1})	A_R (A^4 amu^{-1})
1	gas	2161−2170	1.29−3.93	1.70−20.30	2264−2271	37.00−56.60	4896−6632
	water	2152−2155	0.01−1.13	3.78−39.55	2258−2261	79.14−99.53	11290−14480
	n-hexane	2158−2161	0.86−2.22	2.65−29.37	2262−2266	50.02−66.49	7120−9062
2	gas	2154−2173	9.82−26.72	1.32−46.43	2255−2274	1.10−8.74	3259−7714

[a] To model the water and *n*-hexane environments, the PCM model was applied. Vibrational frequencies are scaled by a factor of 0.960.

is in good agreement with the experimental data because the Raman spectrum of **1** isolated from carrot roots and dissolved in ethanolic solution shows a strong band at 2258 cm^{-1}, but this band is shifted to 2252 cm^{-1} in **2**.[5,34,35] Substantial changes in the theoretical IR intensity and Raman activity of ν_{as}(C≡C) and ν_s(C≡C) modes reflect not only the structural diversity of the conformers but also a sensitivity of these spectroscopic parameters to follow the conformational variation of polyacetylenes that may occur in the living plant tissues. When considering the solvation effect on the conformational equilibria using the polarizable continuum model (PCM),[42] the positions of the ν_{as}(C≡C) and ν_s(C≡C) bands fell into narrower ranges in *n*-hexane and in water than in the gas phase (Table 1). Frequencies of the two modes vary within 3−4 cm^{-1} and are close to the experimental values. In comparison to the gas phase, the ν_s(C≡C) band in water and in *n*-hexane is shifted toward lower wavenumbers by ca. 10 and 3 cm^{-1}, respectively. Furthermore, the IR intensity of the ν_{as}(C≡C) mode decreases in water and in *n*-hexane, whereas that of the ν_s(C≡C) mode increases (Table 1). However, the calculated Raman activities increase up to 3-fold in these solvents, but this has a practical meaning only for the ν_s(C≡C) mode because it is enormously strong. In conclusion, conformational and environmental changes can be responsible only for small shifts even though the former are a few times greater than the environmental ones (Table 1). Nevertheless, when taking into account the solvent influence on polyacetylenes by using the PCM method, it is possible to significantly improve the agreement of the predicted spectroscopic parameters with the experimental ones.

Polyacetylenes in Roots of Wild Carrot. Fresh, unprocessed roots of *D. carota* subsp. *gummifer* and *D. carota* subsp. *maximus* were cut transversally, and Raman signals were recorded from the cut surfaces. The spectra exhibited bands at about 2250 cm^{-1} (Figure 2), which can be assigned to the symmetric stretch of the triple-bond system characteristic of polyacetylenes. The positions of band maxima obtained for individual carrots differ slightly, but they are usually around 2252 cm^{-1}, which is the key band of **2**. Spectra obtained from various root points of all *D. carota* subsp. *maximus* and one *D. carota* subsp. *gummifer* accession show this key band at 2251−2253 cm^{-1}. The results obtained are in good agreement with the previous report for other wild carrots, namely, *D. carota* subsp. *commutatus*, *D. carota* subsp. *maritimus*, and *D. carota* subsp. *gummifer*, where the polyacetylene band was observed at 2253 cm^{-1}.[5] The second *D. carota* subsp. *gummifer* accession measured in this work downshifted the band maximum by 4 cm^{-1} (2248 cm^{-1}). However, it should be noted that the bands recorded from the above-mentioned accessions often also showed slight asymmetry, sometimes even with distinctive broadening (Figure 2D). The detection of asymmetric bands and the fact that band maxima were recorded in the range of a few cm^{-1} may suggest

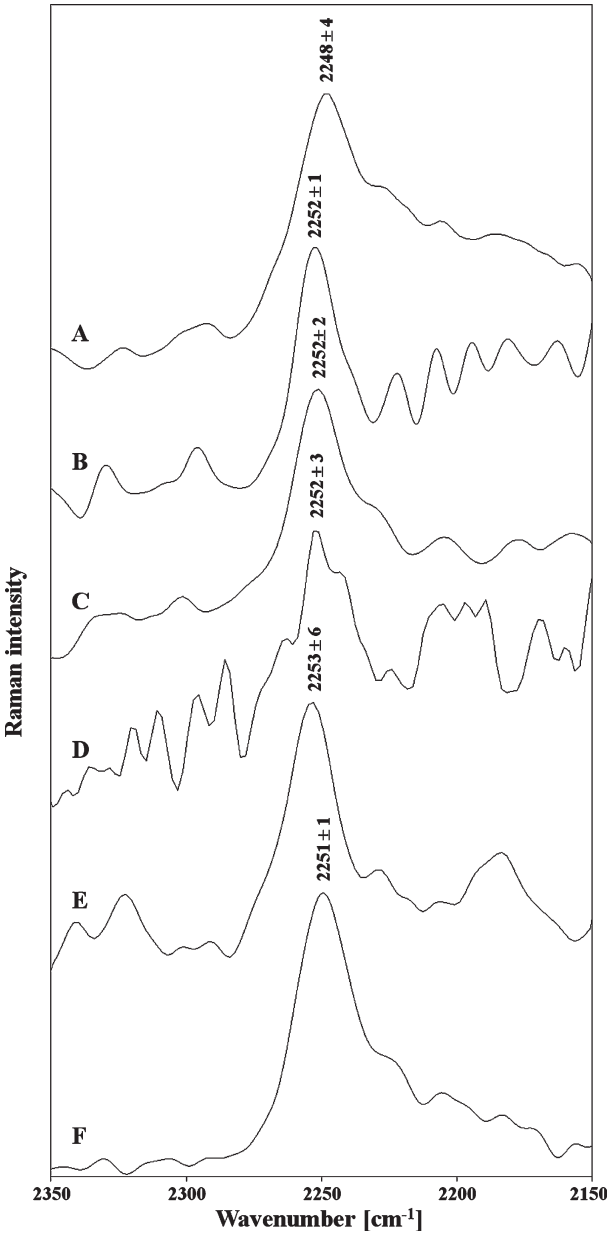

Figure 2. FT-Raman spectra obtained from roots of *D. carota* subsp. *gummifer* (A, B) and *D. carota* subsp. *maximus* (C−F).

the presence of other conformers of **2** or a specific interaction with the plant matrix.

The band at 2258 cm^{-1}, which is characteristic for **1**, was usually not observed. This implies that this compound was either absent in roots or present at a low concentration and likely

dx.doi.org/10.1021/np200265d |*J. Nat. Prod.* 2011, 74, 1757–1763

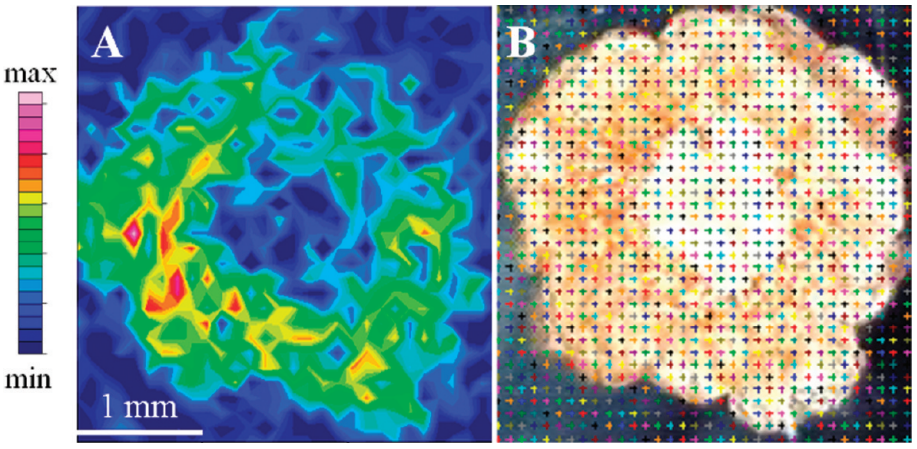

Figure 3. Raman map obtained from a transversely cut *D. carota* subsp. *maximus* root colored according to the band intensity in the spectral region 2220−2280 cm^{-1} (A) and the image of the measured area (B). Mapping parameters: area = 3400 × 3600 μm, increment = 100 μm, laser power = 100 mW, no. of scans per point = 32.

overlapped with the more intense band of **2**. The lower concentration of **1** in comparison to **2** in wild carrot was already determined using chromatography. The ratio of **2**:**1** content was about 17:1 and 4:1 in *D. carota* subsp. *maximus* and *D. carota* subsp. *gummifer* roots, respectively, while only 1.4:1 in *D. carota* subsp. *carota*, although the ratio varied within the taxon depending on the accession.[23,26]

The Raman mapping technique was applied for the assessment of polyacetylene distribution across the root cut surface. Since Raman intensity is proportional to the analyte concentration, the integration of band intensity was applied to demonstrate the quantitative distribution of the component. As seen in Figure 3, the distribution of polyacetylenes is not uniform. The red and purple areas in the map are related to a high concentration of polyacetylenes, while yellow and green ones show low concentrations. Comparing the mapped area to the root image taken by the instrument indicates that high amounts of polyacetylenes occur in the phloem tissue (outer part of the root section), but they are not detectable in the core. Moreover, the Raman map also shows the heterogeneous distribution of polyacetylenes within the phloem tissue. Therefore, higher concentrations of polyacetylenes are restricted to small root fragments only. This pattern of distribution is different from the one reported for *D. carota* subsp. *maritimus*.[5] Although **2** dominated in *D. carota* subsp. *maritimus* phloem, its high concentrations were mainly detected in close proximity to the periderm; however, this was not observed in this study. Here, the distribution of **2** in *D. carota* subsp. *maximus* is more similar to that described for edible carrot.[5]

Starch, Pectin, Cellulose, and Lignin in Roots of Wild Carrot. Several strong bands are observed in the Raman spectrum below 1700 cm^{-1} and can be assigned to specific compounds based on their position.[43] The Raman spectrum measured in a cross section of the *D. carota* subsp. *maximus* root shows the most intense band at 479 cm^{-1} (Figure 4A); this band is characteristic of the skeletal mode of the starch molecule. We confirmed the identity of this band by comparing the spectrum from the root and that of pure starch.[44,45] The strong and intense marker bands due to starch vibrations can be used for the assessment of starch distribution over the root section by using the Raman mapping technique. As shown in Figure 4B, starch is not uniformly distributed; its highest concentration is in the outer part of the phloem tissue. As carrot storage roots develop by periclinal cambial divisions between the xylem and phloem, the phloem cells lying outward are bigger and function as a sink of carbohydrates deposited mainly in the form of nonreducing saccharides.[46] Storage roots usually contain sucrose and reducing sugars, but the presence of starch is less common. In Apiaceae, significant amounts of starch accumulated in *Arracacia xanthorriza*. However, commercial carrots are usually free of starch, except for some white cultivars and wild carrot relatives such as *D. carota* subsp. *maritimus*, where a high level of starch was also observed in the root core.[5,47]

Other strong signals may be attributed to the components of the cell wall. Lignin can be identified by the presence of one or two overlapping bands assigned to two different aromatic ring deformations in the region of 1550−1650 cm^{-1}.[48] In the Raman spectrum of the specimen measured, a strong signal at 1602 cm^{-1} and a shoulder band at 1656 cm^{-1} are present (Figure 4C), confirming the occurrence of lignin. Like the detection of the previous compounds, Raman mapping also visualizes the distribution of lignin over the root section (Figure 4D). The highest levels of lignin occur predominantly in the root core and close to the periderm, but almost no signals were recorded from the phloem tissue. However, the distribution we observed agrees with current knowledge on root anatomy. In roots with secondary growth such as carrot, the core is composed mainly of dead wooden cells with lignified cell walls that strengthen the organ.[46] Also, the periderm that protects the soft parenchymatic storage root may contain partially lignified cells. The presence of lignin accounts for the core being very hard in wild carrot root; understandably, a lower lignin content is desired in commercial edible carrots.

The band at 854 cm^{-1} originates from pectin (Figure 4F). Pectin is a linear polysaccharide containing D-galacturonic acid as the principal constituent; D-galacturonic acid units are linked by α-(1→4) glycosidic bonds. According to the previous reports,[5,43] this band can be assigned to the −C−O−C− skeletal mode of α-anomer carbohydrates. Raman mapping indicates that pectin is present in the outer part of the phloem (Figure 4G), with additional accumulation in the root core.

The characteristic doublet at 1090 and 1124 cm^{-1} (Figure 4H) can be assigned to the asymmetric and symmetric −C−O−C− vibration of the cellulose molecule.[43] Since cellulose is the principal constituent of the plant cell wall, its presence in all tissues should be expected. Examination of the Raman map derived after integration of these doublet bands confirms the presence of cellulose across the

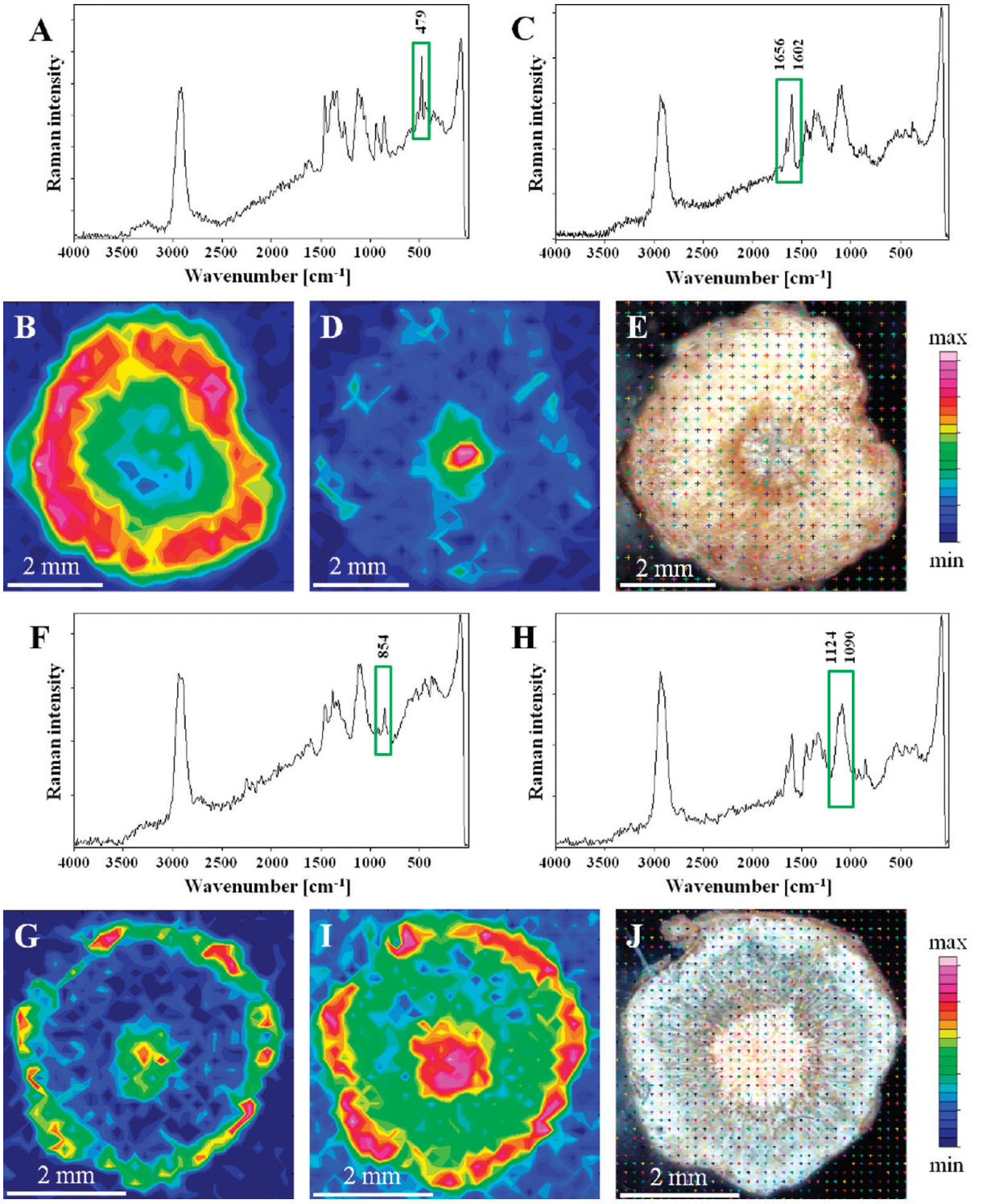

Figure 4. FT-Raman spectra obtained from a transversely cut *D. carota* subsp. *maximus* root with marked characteristic bands and related Raman maps of starch (A, B), lignin (C, D), pectin (F, G), and cellulose (H, I). Mapping parameters for B and D: area = 5980 × 6440 μm, increment = 230 μm, laser power = 100 mW, no. of scans per point = 32; for G and I: area = 4950 × 4950 μm, increment = 150 μm, laser power = 50 mW, no. of scans per point = 64. Digital video images of the measured specimens (E, J).

root section, although its level is much higher in the root core and in the outer part of the phloem (Figure 4I). Secondary root growth causes phloem cells lying outward to be older than the cells close to the cambium. Younger cells have a thin primary cell wall, which is composed of polysaccharides and proteins with sparsely enclosed cellulose fibers. During cell aging, the secondary cell wall is built and more cellulose is incorporated to strengthen the wall. The cell wall growth and thickening cause higher amounts of polysaccharides, including pectin, to be deposited. Thus, the comparison of Raman maps after the integration of the chosen signals shows the changes in

dx.doi.org/10.1021/np200265d |*J. Nat. Prod.* 2011, 74, 1757–1763

the chemical composition of root tissues in relation to secondary growth and reveals higher amounts of pectin and cellulose in older phloem cells. In contrast, Raman maps show that the secondary xylem is composed of cells with lignin and cellulose, but pectin also seems to be present in the parenchymatic xylem cells.

FT-Raman spectroscopy applied here allowed simultaneous investigation of polyacetylenes, lignin, and polysaccharides in the same root sample without a need for the compound extraction. Theoretical quantum chemical calculations, which provided detailed structural analyses of the molecules and predict their spectroscopic properties, were helpful in the interpretation of the observed signal shifts. The calculations indicate that the signal shifts depend on the polyacetylene conformation and the environment in which the molecule is present, i.e., on the plant matrix. Raman mapping visualized a relative content of the compounds measured and provided insight into the chemical composition of intact root tissues. The results revealed a tissue-dependent distribution of polyacetylenes, lignin, and polysaccharides in two wild carrot subspecies and showed that their distribution was different from that found in the previously measured *D. carota* subsp. *maritimus*. In contrast to *D. carota* subsp. *maritimus*, *D. carota* subsp. *maximus* and *D. carota* subsp. *gummifer* develop storage roots containing polyacetylenes in the whole phloem tissue; thus, a big part of the root is a potential source of these bioactive compounds. A lignified, hard xylem tissue of both subspecies is free of polyacetylenes, and its removal should be considered while preparing root material for polyacetylene extraction.

EXPERIMENTAL SECTION

General Experimental Procedures. Raman spectra were recorded using a Bruker MultiRAM FT-Raman spectrometer (coupled with RamanScope III) equipped with a Nd:YAG laser, emitting at 1064 nm, and a germanium detector cooled with liquid nitrogen. The instrument was equipped with an *xy* stage, a mirror objective, and a prism slide for redirection of the laser beam. Root slices were mounted between two glass slides to restrict their movement and avoid deformation during the measurements.

Two-dimensional Raman maps were obtained point by point by moving the *xy* stage; *x* and *y* directions of the accessory were automatically controlled by the spectrometer software. All parameters used for micro-Raman measurements, such as mapping area, step size (increment), laser power, and number of scans for each measured point, are given in the figure captions. All spectra were obtained with a spectral resolution of 4 cm^{-1} in the wavenumber range from 100 to 4000 cm^{-1}. The spectra collected from the mapped areas were smooth corrected and processed by the Bruker Opus/map software package v. 6.5. The maps were obtained by the integration of a specific signal characteristic for the individual analyte and colored according to the Raman intensity.

Calculations. The geometries and harmonic vibrational frequencies of **1** and **2** were calculated by the B3LYP method[36] combined with the Dunning-type aug-cc-pVDZ basis sets[37,38] using the Gaussian 09 program.[39] Conformational analysis was carried out to find the most stable conformers of the investigated compounds. By inspecting the number of imaginary frequencies for each structure, we ensured that only true minima on the potential energy surface were analyzed. Vibrational frequencies obtained from calculations were scaled by a factor of 0.960 to correct for anharmonicity, which was hardly available for a considerable set of quite large molecules, and to improve the agreement with the experimental data.

Biological Material. The plant material comprised six accessions of wild carrot relatives belonging to two *D. carota* subspecies: two accessions of *D. carota* subsp. *gummifer* (Nos. DAL13/96Pop and 964/92-2 EPN from the Julius Kuehn Institute, Quedlinburg, Germany, JKI) and four accessions of *D. carota* subsp. *maximus* (No. DAU/257 from the Leibnitz Institute of Plant Genetics and Plant Crop Research, Gatersleben, Germany; No. GRCGGB/11022 from the Greek Gene Bank, Thessaloniki, Greece; No. 288-1 from the United States Department of Agriculture, Madison, WI, USA, and No. DAL18/96Pop from JKI). The seeds were sown in soil in pots, and the plants were grown in a glasshouse. The roots were harvested after their development and used for spectroscopic measurements directly.

AUTHOR INFORMATION

Corresponding Author

*Tel: +48 12 6625191. Fax: +48 12 4119043. E-mail: baranski@ogr.ur.krakow.pl.

ACKNOWLEDGMENT

The authors thank Prof. P. W. Simon (USDA-ARS, Madison, WI, USA), Dr. T. Nothnagel (JKI, Quedlinburg, Germany), and the curators of *Daucus* collections in the Greek and German gene banks for their generous seed supply. The authors also thank the Academic Computer Centre CYFRONET AGH, Kraków, Poland, for providing computing time. This research was supported by the International Ph.D. studies program at the Faculty of Chemistry, Jagiellonian University, within the Foundation for Polish Science MPD Program co-financed by the EU European Regional Development Fund. We also gratefully acknowledge the support of the Polish Ministry of Science and Higher Education (Grant No. MNiSW 97/N-DFG/2008/0).

REFERENCES

(1) Heywood, V. H. *Isr. J. Bot.* **1983**, *32*, 51–65.
(2) Sáenz Laín, C. *An. Jardín Bot. Madrid* **1981**, *37*, 481–534.
(3) Crowden, R. K.; Harborne, J. B.; Heywood, V. H. *Phytochemistry* **1969**, *8*, 1963–1984.
(4) Hegnauer, R. Chemical Patterns and Relationships of Umbelliferae. In *The Biology and Chemistry of the Umbelliferae*; Heywood, V. H., Ed.; Academic Press: London, 1971; pp 267−277.
(5) Baranska, M.; Schulz, H.; Baranski, R.; Nothnagel, T.; Christensen, L. P. *J. Agric. Food Chem.* **2005**, *53*, 6565–6571.
(6) Calabrese, E. J.; Baldwin, L. A. *Environ. Health Persp.* **1998**, *106*, 357–362.
(7) Young, J. F.; Duthie, S. J.; Milne, L.; Christensen, L. P.; Duthie, G. G.; Bestwick, C. S. *J. Agric. Food Chem.* **2007**, *55*, 618–623.
(8) Brandt, K.; Christensen, L. P.; Hansen-Møller, J.; Hansen, S. L.; Haraldsdóttir, J.; Jespersen, L.; Purup, S.; Kharazmi, A.; Barkholt, V.; Frøkiær, H.; Kobæk-Larsen, M. *Trends Food Sci. Technol.* **2004**, *15*, 384–393.
(9) Harding, V. K.; Heale, J. B. *Physiol. Plant Pathol.* **1981**, *18*, 7–15.
(10) Garrod, B.; Lewis, B. G.; Coxon, D. T. *Physiol. Plant Pathol.* **1978**, *13*, 241–246.
(11) Appendino, G.; Tagliapietra, S.; Nano, G. M. *Fitoterapia* **1993**, *64*, 179.
(12) Kuo, S. C.; Teng, C. M.; Lee, J. C.; Ko, F. N.; Chen, S. C.; Wu, T. S. *Planta Med.* **1990**, *56*, 164–167.
(13) Kobaisy, M. Z.; Abramowski, Lermer, L.; Saxena, G.; Hancock, R. E. W.; Towers, G. H. N.; Doxsee, D.; Stokes, R. W. *J. Nat. Prod.* **1997**, *60*, 1210–1213.
(14) Lee, S. W.; Kim, K.; Rho, M. C.; Chung, M. Y.; Lee, H. S.; Kim, Y. K. *Planta Med.* **2004**, *70*, 197–200.
(15) Wang, C. N.; Shiao, Y. J.; Kuo, Y. H.; Chen, C. C.; Lin, Y. L. *Planta Med.* **2000**, *66*, 644–647.
(16) Metzger, B. T.; Barnes, D. M.; Reed, J. D. *J. Agric. Food Chem.* **2008**, *56*, 3554–3560.

(17) Kwon, B. M.; Nam, J. Y.; Lee, S. H.; Jeong, T. S. *Chem. Pharm. Bull.* **1996**, *44*, 444–445.
(18) Kim, Y. S.; Kim, S. I.; Hahn, D. R. *Saengyak Hakhoechi* **1989**, *20*, 154–161.
(19) Matsunaga, H.; Katano, M.; Yamamoto, H.; Fujito, H.; Mori, M.; Takata, K. *Chem. Pharm. Bull.* **1990**, *K.38*, 3480–3482.
(20) Bernart, M. W.; Cardellina, J. H. II; Balaschak, M. S.; Alexander, M.; Shoemaker, R. H.; Boyd, M. R. *J. Nat. Prod.* **1996**, *59*, 748–753.
(21) Czepa, A.; Hofmann, T. *J. Agric. Food Chem.* **2003**, *51*, 3865–873.
(22) Czepa, A.; Hofmann, T. *J. Agric. Food Chem.* **2004**, *52*, 4508–4514.
(23) Metzger, B. T.; Barnes, D. M. *J. Agric. Food Chem.* **2009**, *57*, 11134–11139.
(24) Olsson, K.; Svensson, R. *Phytopathol. J.* **1996**, *144*, 441–447.
(25) Pferschy-Wenzig, E. M.; Getzinger, V.; Kunert, O.; Woelkart, K.; Zahrl, J.; Bauer, R. *Food Chem.* **2009**, *114*, 1083–1090.
(26) Schulz-Witte J. Diversität Wertgebender Inhaltsstoffe bei *Daucus carota* L. Dis. Julius Kühn Inst. Quedlinburg 2010, available via http://www.jki.bund.de. Cited Jul 5, 2011.
(27) Ng, A.; Waldron, K. W. *J. Sci. Food Agric.* **1997**, *73*, 503–512.
(28) Christensen, L. P.; Brandt, K. *J. Pharm. Biomed. Anal.* **2006**, *41*, 683–693.
(29) Zidorn, C.; Johrer, K.; Ganzera, M.; Schubert, B.; Sigmund, E. M.; Mader, J.; Greil, R.; Ellmerer, E. P.; Stuppner, H. *J. Agric. Food Chem.* **2005**, *53*, 2518–2523.
(30) de Oliveira, V. E.; Castro, H. V.; Edwards, H. G. M.; de Oliveira, L. F. C. *J. Raman Spectrosc.* **2010**, *41*, 642–650.
(31) Edwards, H. G. M.; Farwell, D. W.; de Oliveira, L. F. C.; Alia, J. M.; Le Hyaric, M.; de Ameida, M. V. *Anal. Chim. Acta* **2005**, *532*, 177–186.
(32) Baranska, M.; Schulz, H.; Krüger, H.; Quilitzsch, R. *Anal. Bioanal. Chem.* **2005**, *381*, 1241–1247.
(33) Schrader, B.; Schulz, H.; Baranska, M.; Andreev, G. N.; Lehner, C.; Sawatzki, J. *Spectrochim. Acta A* **2005**, *61*, 1395–1401.
(34) Baranska, M.; Schulz, H. *Analyst* **2005**, *130*, 855–859.
(35) Baranska, M.; Schulz, H.; Christensen, L. P. *J. Agric. Food Chem.* **2006**, *54*, 3629–3635.
(36) Becke, A. D. *J. Chem. Phys.* **1993**, *98*, 5648–5652.
(37) Dunning, T. H., Jr. *J. Chem. Phys.* **1989**, *90*, 1007–1023.
(38) Kendall, R. A.; Dunning, T. H.; Harrison, R. J. *J. Chem. Phys.* **1992**, *96*, 6796–6806.
(39) Frisch, M. J.; Trucks, G. W.; Schlegel, H. B.; Scuseria, G. E.; Robb, M. A.; Cheeseman, J. R.; Scalmani, G.; Barone, V.; Mennucci, B.; Petersson, G. A.; Nakatsuji, H.; Caricato, M.; Li, X.; Hratchian, H. P.; Izmaylov, A. F.; Bloino, J.; Zheng, G.; Sonnenberg, J. L.; Hada, M.; Ehara, M.; Toyota, K.; Fukuda, R.; Hasegawa, J.; Ishida, M.; Nakajima, T.; Honda, Y.; Kitao, O.; Nakai, H.; Vreven, T.; Montgomery, Jr. J. A.; Peralta, J. E.; Ogliaro, F.; Bearpark, M.; Heyd, J. J.; Brothers, E.; Kudin, K. N.; Staroverov, V. N.; Kobayashi, R.; Normand, J.; Raghavachari, K.; Rendell, A.; Burant, J. C.; Iyengar, S. S.; Tomasi, J.; Cossi, M.; Rega, N.; Millam, J. M.; Klene, M.; Knox, J. E.; Cross, J. B.; Bakken, V.; Adamo, C.; Jaramillo, J.; Gomperts, R.; Stratmann, R. E.; Yazyev, O.; Austin, A. J.; Cammi, R.; Pomelli, C.; Ochterski, J. W.; Martin, R. L.; Morokuma, K.; Zakrzewski, V. G.; Voth, G. A.; Salvador, P.; Dannenberg, J. J.; Dapprich, S.; Daniels, A. D.; Farkas, O.; Foresman, J. B.; Ortiz, J. V.; Cioslowski, J.; Fox, D. J. *Gaussian 09*, Revision A.1; Gaussian Inc.: Wallingford, CT, 2009.
(40) Roman, M.; Dobrowolski, J. Cz.; Baranska, M. *J. Chem. Inf. Model.* **2011**, *51*, 283–295.
(41) Roman, M.; Baranska, M. *Spectroscopy* **2010**, *3−4*, 417–420.
(42) Tomasi, J.; Mennucci, B.; Cammi, R. *Chem. Rev.* **2005**, *105*, 2999–3094.
(43) Schulz, H.; Baranska, M. *Vib. Spectrosc.* **2007**, *43*, 13–25.
(44) Thygesen, L. G.; Løkke, M. M.; Micklander, E.; Engelsen, S. B. *Trends Food Sci. Technol.* **2003**, *14*, 50–57.
(45) Dupuy, N.; Laureyns, J. *Carbohydr. Polym.* **2002**, *49*, 83–90.
(46) Esau, K. *Hilgardia* **1940**, *13*, 175–225.
(47) Santacruz, S.; Ruales, J.; Eliasson, A.-C. *Carbohydr. Polym.* **2003**, *51*, 85–92.
(48) Larsen, K. L.; Barsberg, S. *J. Phys. Chem. B* **2010**, *114*, 8009–8021.